Journal of Applied Polymer Science

Crystallization and mechanical behavior of covalent functionalized carbon nanotube/poly(3-hydroxybutyrate-*co*-3-hydroxyvalerate) nanocomposites

Ni Jiang, Hideki Abe
Bioplastic Research Team, Biomass Engineering Program Cooperation Division, RIKEN Center for Sustainable Resource Science, Wako-shi, Saitama 351-0198, Japan
Correspondence to: H. Abe (E-mail: habe@riken.jp)

ABSTRACT: To improve the dispersity of multi-walled carbon nanotubes (MWCNTs) in poly(3-hydroxybutyrate-*co*−3-hydroxyvalerate) (PHBV) matrix, MWCNTs functionalized with carboxyl groups, hydroxyl groups, and atactic poly (3-hydroxybutyrate) (ataPHB) through acid oxidation, esterification reaction, and "grafting from" method, respectively, were used to fabricate nanofiller/PHBV nanocomposites. The crystallization behavior, dispersion of MWCNTs before and after functionalization in PHBV matrices, and mechanical properties of a series of nanocomposites were investigated. The differential scanning calorimetry, wide-angle X-ray diffraction, and polarized optical microscope results suggested that the four types of MWCNTs acted as effective heterogeneous nucleation agents, inducing an increase in the crystallization rate, crystallinity, and crystallite size. Scanning electron microscope observations demonstrated that functionalized MWCNTs showed improved dispersion comparing with MWCNTs, suggesting an enhanced interfacial interaction between PHBV and functionalized MWCNTs. Consequently, the mechanical properties of the functionalized MWCNTs/PHBV nanocomposites have been improved as evident from dynamic mechanical and static tensile tests. © 2015 Wiley Periodicals, Inc. J. Appl. Polym. Sci. **2015**, *132*, 42136.

KEYWORDS: composites; crystallization; functionalization of polymers; nanotubes

Received 11 December 2014; accepted 20 February 2015
DOI: 10.1002/app.42136

INTRODUCTION

Polyhydroxyalkanoates (PHAs) are a family of aliphatic polyesters produced by bacteria as an intracellular material to store carbon and energy.[1,2] PHAs are potential substitutes to petroleum-based synthetic polymers due to their complete biodegradability, biocompatibility, natural origin, and physical and mechanical properties which are similar to conventional thermoplastics. One of the most extensively studied member of PHAs family is poly(3-hydroxybutyrate-*co*-3-hydroxyvalerate) (PHBV), whose physical properties are strongly affected by the molar fraction of 3-hydroxyvalerate.[3] Compared with homopolymer poly(3-hydroxybutyrate) (PHB), the mechanical properties of PHBV have been enhanced. In addition, the lower melting temperature (T_m) of semi-crystalline PHBV offers the possibility of processing at lower temperatures.[4] Unfortunately, the application of PHBV is hindered by some disadvantages such as slow crystallization rate and interlamellar secondary crystallization on storage.[5] What's more, PHBV has a low degree of heterogeneous nucleation density for the much high purity, which induces the low elongation at break. Therefore, the expansion of commercial applications for PHBV will necessitate the improvement of the crystallization and processing behavior, and the enhancement of the mechanical properties. It is known that preparing PHBV nanocomposite is one of the easiest methods to improve the properties of PHBV.[6–8]

Carbon nanotubes (CNTs) have attracted much attention of academic and industrial researchers because of their fascinating physical properties and unique structures since their discovery by Iijima in 1991.[9] They are one-dimensional entities with an extremely high aspect ratio and surface area, thus only a little amount of CNTs can remarkably improve the property of polymers. Therefore, CNTs are one of the most promising candidates for the modification of polymers.[10,11] However, homogeneous dispersion without aggregation in a polymer matrix is extremely difficult for CNTs because they usually form stable bundles due to Van der Waals interactions. In addition, good interfacial adhesion between CNTs and polymers is essential for property improvement of the composite. But the

Additional Supporting Information may be found in the online version of this article.

nonreactive nature of CNTs would lead to a weak interfacial interaction with the polymer matrix and resulted in phase separation. Polymer grafting of carbon nanotubes is an efficient way to achieve a homogeneous dispersion of nanotubes in the polymer matrix and excellent interfacial stress transfer between nanotubes and polymer.[12] However, due to the relative smooth graphene like surface of nanotubes, there is a lack of interfacial bonding between CNTs and polymer matrix. Therefore, chemical functionalization of the nanotube surface is necessary, and it is frequently initiated by introducing carboxyl groups on the surface of CNTs with an acid oxidation method.[13]

Even though increasing attention has been given to the fabrication and the property studies of CNTs/polymer nanocomposites due to the remarkably enhanced physical properties of the composites, the research on PHBV nanocomposites based on covalent functionalized CNTs, especially PHB grafted CNTs, has rarely been a concern in the past investigations. It was reported that the synthetic analog of natural PHB with various tacticities (atactic, isotactic, and syndiotactic) can be prepared by ring opening polymerization of β-butyrolactone (β-BL) using various types of catalysts.[14–17] Also, fully amorphous atactic PHB (ataPHB) is miscible with bacterial PHBV in the melt as reported by Scandola.[18] Therefore, ataPHB was one of the best choices for the grafting of CNTs to improve the dispersity and interfacial adhesion between CNTs and PHBV.

In this study, to improve the crystallization and mechanical properties of PHBV, three types of covalent functionalized multiwalled carbon nanotubes (MWCNTs) (carboxyl-functionalized (MWCNTs-COOH), hydroxyl-functionalized (MWCNTs-OH), and ataPHB-functionalized (MWCNTs-PHB) were used to fabricate nanofiller/PHBV nanocomposites. The thermal properties, crystallization, and mechanical behavior of these nanocomposites were studied and compared with MWCNTs/PHBV nanocomposite in detail by differential scanning calorimetry (DSC), wide-angle X-ray diffraction (WAXD), polarized optical microscopy, tensile test, and dynamic mechanical analysis (DMA).

EXPERIMENTAL

Materials

PHBV with HV content, M_n, and polydispersity of 12 mol %, 1.49×10^5, and 2.3, respectively, is produced by ICI, Agricultural Division, Billingham, UK, and is available under the trade name Biopol. PHBV was purified by dissolving in chloroform at 80°C and then precipitating from methanol. The MWCNTs with diameter of 10–30 nm and length of 5–15 μm were purchased from Tokyo Chemical Industry (TCI). Racemic β-butyrolactone (β-BL), 3-ethyl-3-oxetanemethanol, and *o*-dichlorobenzene (ODCB) were dried by calcium hydride (CaH_2) and magnesium sulfate ($MgSO_4$), respectively, and then distilled under reduced pressure. Stannous octoate ($SnOct_2$) purchased from Aldrich Chemical was dissolved in distilled *o*-dichlorobenzene prior to use. Other materials were used without further purification.

Preparation of MWCNTs-COOH

MWCNTs were mixed with sulfuric acid and nitric acid (3 : 1 in volume), treated in ultrasonic bath for 1 h, and then refluxed at 80°C for 6.5 h to obtain the MWCNTs-COOH. The excess acids were washed thoroughly with deionized water until the pH value was about 7.0. MWCNTs-COOH were dried and ground to powder in an agate mortar.

Preparation of MWCNTs-OH

After the drying of MWCNTs-COOH and catalyst tetraphenylphosphonium bromide (TPPB) in a reaction tube under vacuum, dehydrate dimethyl sulfoxide (DMSO) was added under nitrogen and then sonicated for 2 h. After the addition of a certain amount of 3-ethyl-3-oxetanemethanol into the suspension, the tube was immersed into an oil bath setting at 160°C and stirred for 80 h. The reaction mixture was cooled and precipitated from excess methanol. The obtained products were filtrated with 0.2 μm PTFE millipore membrane under reduced pressure and dried under vacuum.

Preparation of MWCNTs-PHB

After the drying of MWCNTs-OH in a reaction tube under vacuum, racemic β-BL and ODCB solution of stannous octoate were added to the tube under nitrogen, and the reaction was performed at 130°C under refluxing condition for 80 h. The reaction mixture was cooled and precipitated from excess methanol. The obtained products were filtrated with 0.2 μm PTFE millipore membrane under reduced pressure and washed with chloroform several times to remove the free and physically absorbed ataPHB and then dried under vacuum.

Preparation of Nanofiller/PHBV Nanocomposites

To obtain a homogeneous dispersion of nanofillers in the polymer matrix, nanofiller/PHBV nanocomposites with the nanofiller content ranging from 0 to 3.0 wt % were prepared in two steps: solution mixing to disaggregate the nanofillers and then melt mixing the dried mixture to overcome partial sedimentation. The detailed process was as follows: nanofillers were ultrasonically dispersed in $CHCl_3$ for 1 h, and then PHBV was added to the suspension and stirred for a certain time to ensure sufficient mixing. After ultrasonic for another 10 min, the suspension was poured into glass Petri dishes for solvent evaporation. The residual trace solvent was removed under vacuum overnight. The dried film was then melt extruded at 165°C with a screw speed of 50 rpm, the mixing process continued for 3 min. The extrudates were sandwiched between two Teflon films with another 0.1-mm-thick Teflon film as spacer and compressed at 180°C, and then isothermal crystallized at ambient temperature over 3 days before use. The pure PHBV sample was also processed under the same condition for comparison.

Characterizations

Thermal gravimetric analysis (TGA) was performed at a heating rate of 10°C/min under nitrogen atmosphere. Raman measurements were performed on a Raman spectroscope instrument (JASCO NRS-2100) equipped with an Ar ion laser (632.8 nm) as excitation source. DSC data were recorded in the temperature range −30 to 200°C on a Perkin Elmer DSC8500 equipped with a liquid nitrogen cooling accessory under a nitrogen flow of 20 mL/min. For the measurement of T_m, the samples after isothermal crystallization at ambient temperature over 3 days were heated from −30 to 200°C at a heating rate of 20°C/min. To

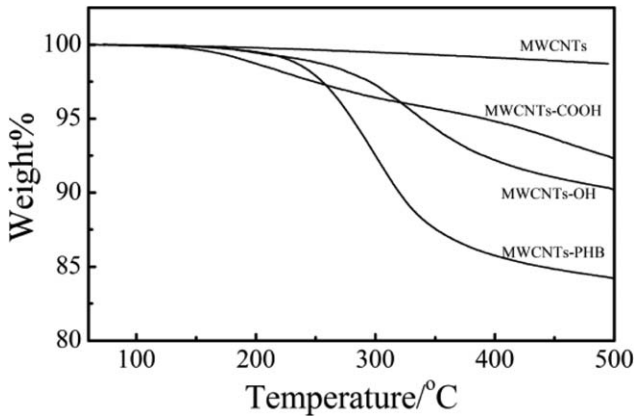

Figure 1. TGA curves of pristine MWCNTs and functionalized MWCNTs. The heating rate is 10°C/min and under N_2 atmosphere.

determine the non-isothermal crystallization temperature (T_p), the samples were maintained at 200°C for 30 s, and then cooled to −10°C at a cooling rate of 10°C/min. With respect to isothermal crystallization, after melting at 200°C for 30 s, the samples were rapidly quenched to a given temperature and held for a certain time. The WAXD patterns of these films were recorded at room temperature on a Rigaku RINT2500 diffractometer with a nickel-filtered Cu Kα radiation (wavelength $\lambda = 0.154$ nm, 40 kV and 100 mA) in the 2θ range of 5–35° with a scanning step of 0.02° and a scanning rate of 1°/min. An Olympus BX51 microscope with DP21 digital camera was used in this study to observe spherulitic morphology. The dispersion of nanofillers in the fractured surfaces of nanofiller/PHBV nanocomposites (fractured in liquid nitrogen) was observed with a scanning electron microscope (SEM) (JEOL JSM-6330F) after gold coating of the films using an ion coater. Dynamic mechanical analysis (DMA) was performed with a DMA 8000 from PerkinElmer. A dual cantilever clamp was used at the frequency of 0.6 Hz. The samples were heated from −100 to 100°C at a heating rate of 5°C/min. Tensile tests were performed on a Shimadzu autograph AG-X plus series tensile testing machine with a crosshead speed of 5 mm/min and an initial gauge length of 15 mm at room temperature. The sample films, with a thickness of about 0.2 mm, were cut into strips with a width of 10 mm. At least three strips were measured for each sample.

RESULTS AND DISCUSSION

Preparation and Characterization of Functionalized MWCNTs

Considering the nonreactive nature of MWCNTs, to realize the covalent functionalization of nanotubes, carboxyl groups were first introduced onto the surface of MWCNTs by acid oxidation, and then converted into hydroxyl groups by reacting with 3-ethyl-3-oxetanemethanol. To introduce atactic PHB on the surface of MWCNTs, MWCNTs-OH was used to initiate the ring-opening polymerization of racemic β-BL with the presence of $SnOct_2$, as shown in Supporting Information Scheme S1. After the grafting reaction, the products were washed thoroughly with chloroform to remove any chloroform-soluble substances (such as PHB) unbound to the MWCNTs.

The amounts of —OH and PHB grafted on the surface of MWCNTs were determined through the TGA analysis. Figure 1 shows the TGA curves of pristine MWCNTs, MWCNTs-COOH, MWCNTs-OH, and MWCNTs-PHB under nitrogen atmosphere. MWCNTs hardly decomposed below 500°C and about 98.7 wt % remained at 500°C. However, the mass losses of 7.7 wt %, 9.8 wt %, and 15.8 wt % for MWCNTs-COOH, MWCNTs-OH, and MWCNTs-PHB, respectively, were observed at 500°C. The weight loss of MWCNTs-COOH demonstrates the formation of thermally unstable functional groups (e.g., carboxyl groups) on the surface of MWCNTs during the oxidation process. The difference in weight loss (ΔW) at 500°C between MWCNTs-COOH and MWCNTs-OH mainly results from the reaction with of 3-ethyl-3-oxetanemethanol ($M_n = 116$). Therefore, it could be roughly estimated that the amount of introduced —OH groups is about 0.6 wt % (—OH amount = $\Delta W \times 17 \times 2/116$). Although the ΔW between MWCNTs-OH and MWCNTs-PHB is mainly from the introduced ataPHB, indicating that the amount of grafted ataPHB is about 6.0 wt %.

Raman spectroscopy has been a sensitive probe of the electronic structure in carbon nanotubes and presence of defects. The Raman spectra shown in Figure 2 revealed that the *D*- and *G*-bands are at 1351 and 1572 cm^{-1}, respectively, for all MWCNTs materials. The disorder *D*-band in pristine MWCNTs indicates the presence of a small number of sp^3-hybridized carbons within the nanotube framework. The *D*/*G* band ratio increased from about 0.84 in the pristine MWCNTs to approximately 1.04 in the acid oxidized compounds. This result suggests that the acid oxidation treatment introduced a substantial amount of defects like carboxyl groups at the MWCNTs sidewalls. Upon further reacting with 3-ethyl-3-oxetanemethanol and β-BL, the disorder bands in the spectrum were a little weakened with respect to *G* bands, which probably because the molecules attached to the sidewall hindered the radial breathing and disorder oscillation motion. All in all, the increased *D*/*G* band ratio for all functionalized MWCNTs confirmed the successful covalent modification.

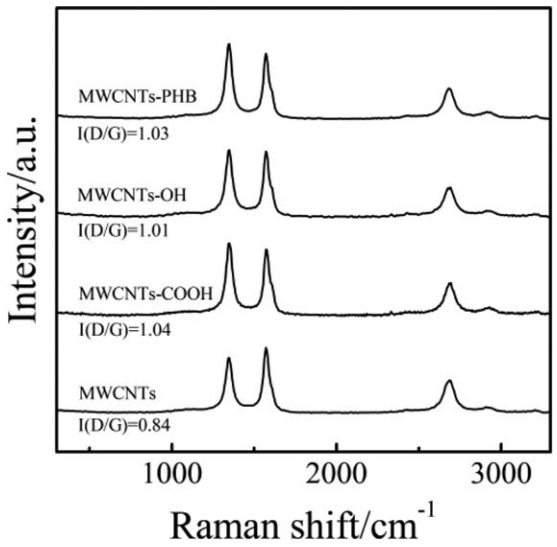

Figure 2. Raman spectra of pristine MWCNTs and functionalized MWCNTs.

Table I. The Calculated DSC Thermal Data and X-ray Crystallinity of PHBV and Its Nanocomposites

Sample	Nanofiller content	T_{m1} (°C)	T_{m2} (°C)	ΔH_m (J/g)	T_p (°C)	ΔH_c (J/g)	X_t (%)
PHBV	0%	134.1	150.7	62.3	58.4	−18.6	68.9
MWCNTs/PHBV nanocomposite	0.1%	135.5	153.0	58.0	61.9	−40.3	67.5
	0.6%	135.8	152.1	57.1	77.4	−42.7	74.5
	1.0%	136.3	151.5	58.3	71.7	−45.5	73.8
	3.0%	137.6	153.4	53.8	83.6	−45.4	77.3
MWCNTs-PHB/PHBV nanocomposite	0.1%	134.2	149.4	58.9	56.4	−37.3	66.3
	0.6%	135.5	151.5	55.1	71.8	−39.2	64.3
	1.0%	134.7	151.4	53.0	55.1	−37.4	70.3
	3.0%	132.2	148.1	50.2	55.3	−39.2	72.1

Melting and Crystallization Behavior of Nanocomposites

PHBV is a typical semicrystalline polymer. Both processing and physical properties of this polymer greatly depend on its T_m, crystallization rate, crystallinity, and solid-state morphology. Therefore, it is important to study the influence of nanofillers on the melting and crystallization behavior of the polymer matrix. As the melting curves of all nanocomposites were similar, only the results for nanocomposites with 1.0 wt % nanofiller loading are shown in Supporting Information Figure S1. The low-melting peak temperature (T_{m1}), high-melting peak temperature (T_{m2}), and melting enthalpy (ΔH_m) of neat PHBV, MWCNTs/PHBV, and MWCNTs-PHB/PHBV nanocomposites are listed in Table I. All samples showed obvious double melting peaks with the high temperature peak as the dominant one. This complex double melting behavior is due to the melting–recrystallization–remelting mechanism during heating.[19] As shown in Table I, the T_{m1} of MWCNTs/PHBV nanocomposite increased slightly with an increase in MWCNTs content whereas the T_{m2} was more or less unchanged, implying that the heterogeneous nucleation induced more perfect crystals. For MWCNTs-PHB/PHBV nanocomposite, the T_{m1} first slightly increased and then decreased, which might be ascribed to the two opposite effects. On one hand, MWCNTs-PHB acted as nucleating agents and induced more perfect crystals. On the other hand, the amorphous ataPHB grafted on the surface of MWCNTs confined the crystallization of PHBV main chain and induced imperfect crystals.

The non-isothermal crystallization exotherms of neat PHBV and nanofiller/PHBV nanocomposites during cooling from the melt at 10°C/min are presented in Figure 3. It was apparent that the onset crystallization temperature (T_0) of all nanocomposites shifted to higher temperatures compared with neat PHBV, indicating that all nanofillers behave as nucleating agents for the crystallization of PHBV. In the case of MWCNTs-OH, the crystallization peak was wide and the T_0 was higher than other nanocomposites when the contents of nanofillers are 0.6 wt % and 1.0 wt %. Maybe this results from the small amount of —OH groups on the surface of MWCNTs which could form hydrogen bonds with the C═O groups in PHBV matrix, this facilitates the nucleation of PHBV. In addition, the crystallization enthalpies (ΔH_c) of nanocomposites were much higher than that of neat PHBV, implying that nanofillers are beneficial to the crystallization of PHBV and greatly enhance the crystallinity of the nanocomposites. Similar phenomenon of the increase in ΔH_c with the addition of nanofiller was observed by Yang *et al.*[20] The T_p of nanocomposites during cooling was a little complicate. In general, the T_p of all nanocomposites shifted toward higher temperature at first and reached maximum with a nanofiller content of 0.6 wt %, and subsequently shifted toward lower temperature and then increased again with the increasing of nanofiller contents. Also, it was found that the effects of functionalized MWCNTs on the non-isothermal crystallization of PHBV are similar, which is much different from MWCNTs. Therefore, the T_p and ΔH_c of neat PHBV, PHBV/MWCNTs, and PHBV/MWCNTs-PHB nanocomposites are listed in Table I for comparison. As shown in Table I, the T_p of PHBV increased dramatically (from 58.4°C to 61.9°C) even with the addition of only 0.1 wt % MWCNTs, indicating an obvious nucleation effect of MWCNTs.[21] The T_p value decreased as the MWCNTs content increasing to 1.0 wt % but increased again with further addition of MWCNTs. The effect of MWCNTs-PHB on the non-isothermal crystallization temperature of PHBV was much weaker but the same trend as MWCNTs. The results suggest that the imperfect surface of functionalized MWCNTs is unfavorable for the heterogeneous nucleation of PHBV. Additionally, the T_p of MWCNTs-PHB/PHBV nanocomposite was lower than other two functionalized MWCNTs/PHBV nanocomposites as shown in Figure 3, which was resulted from the restriction effect of ataPHB on the crystallization of PHBV. The complicate effect of nanofiller content on the T_p of PHBV matrix could be attributed to the synergy of following factors. First, the number of nucleation sites increases with increasing nanofiller content, which is favorable for the crystallization of PHBV. Second, further addition of nanofillers might induce agglomeration of nanofillers in nanocomposites, which results in decreasing amount of heterogeneous nucleation sites. Third, more steric hindrance introduced by nanofillers limits the mobility of PHBV chains which is not favorable to the crystallization. The ΔH_c of MWCNTs-PHB/PHBV

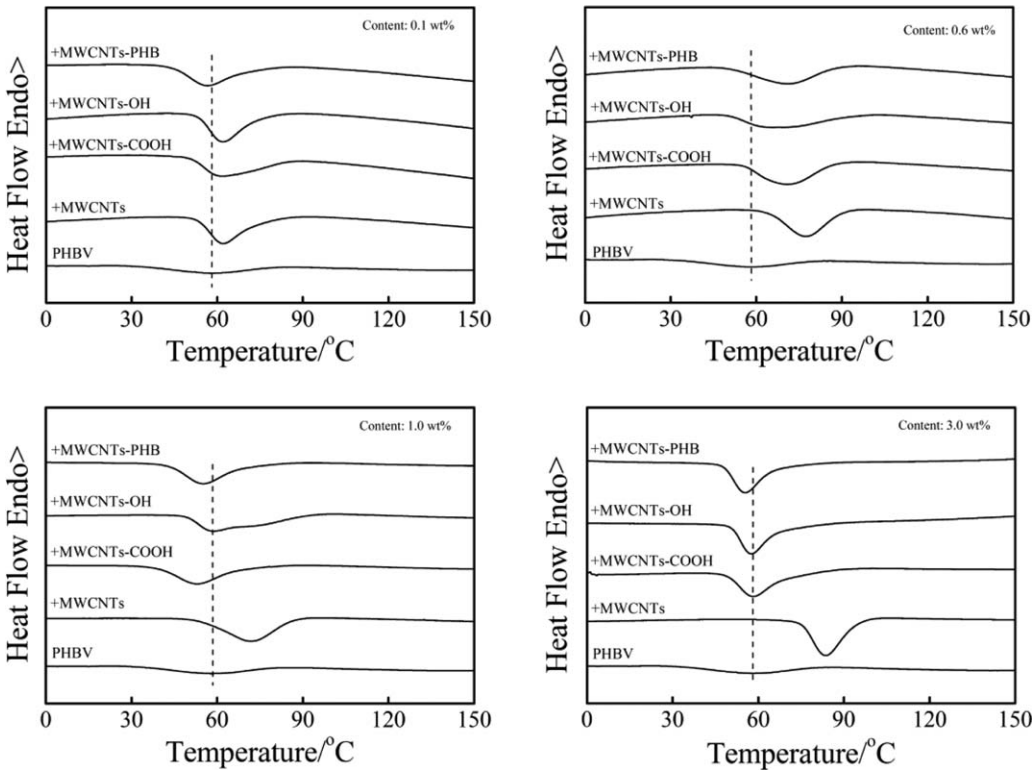

Figure 3. The non-isothermal crystalline curves of PHBV and its nanocomposites with different contents of nanofillers at a cooling rate of 10°C/min.

nanocomposite was lower than that of MWCNTs/PHBV nanocomposite, indicating a lower crystallinity of the former. This phenomenon is resulted from the confinement of ataPHB on PHBV matrix, which is in consistent with the melting results. The isothermal crystallization of PHBV and its nanocomposites were investigated to give more detailed information on the effect of nanofillers on the crystallization of PHBV matrix. The crystallization half-time ($t_{1/2}$) of the isothermal DSC curves are plotted as a function of isothermal crystallization temperature (T_c) for PHBV, MWCNTs/PHBV, and MWCNTs-PHB/PHBV nanocomposites, and the results are shown in Figure 4. Crystallization half-time $t_{1/2}$ is defined as the time at which the extent of crystallization is 50%. It was observed that neat PHBV showed a typical bell-shaped curve with the minimum at about 60°C, while nanocomposites also showed bell-shaped curves but the minimum $t_{1/2}$ values a little moved to lower temperatures. The $t_{1/2}$ of PHBV nanocomposites decreased dramatically within the temperature range of our DSC experiments, suggesting the greatly increased crystallization rate, that is, strong nucleation effects of nanofillers. Also, same trend of $t_{1/2}$ versus contents of nanofiller for all nanofiller/PHBV nanocomposites was found, $t_{1/2}$ increased at first and subsequently decreased and then increased again with the increasing of nanofiller content. It is well consistent with the observations from non-isothermal process. The comparison results (Figure 4) also indicate the weaker nucleation effects of MWCNTs-PHB than MWCNTs as

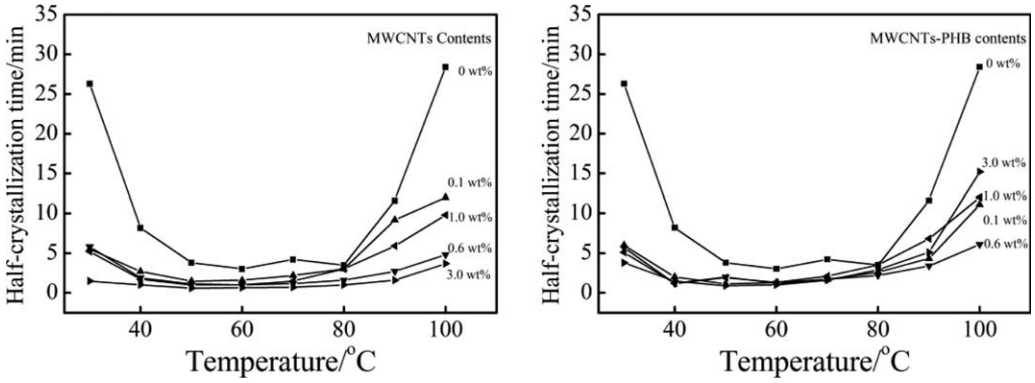

Figure 4. Crystallization half-time of MWCNTs/PHBV and MWCNTs-PHB/PHBV nanocomposites as a function of isothermal crystallization temperature.

Table II. The Calculated X-ray *d* Spacings, Crystallite Sizes, and Crystallinity of PHBV and Its Nanocomposites with Nanofiller Content of 1.0 wt %

Sample	*h k l*	2θ (°)	*d* spacing (Å)	F_{WHM}	H_{hkl} (nm)	X_t (%)
PHBV	020	13.20	6.70	0.394	21.6	68.9
	110	16.62	5.33	0.415	20.9	
MWCNTs/PHBV nanocomposite	020	13.36	6.62	0.332	25.7	73.8
	110	16.76	5.29	0.385	22.5	
MWCNTs-COOH/PHBV nanocomposite	020	13.26	6.67	0.326	26.2	73.4
	110	16.66	5.32	0.395	21.9	
MWCNTs-OH/PHBV nanocomposite	020	13.32	6.64	0.389	21.9	65.5
	110	16.74	5.29	0.417	20.8	
MWCNTs-PHB/PHBV nanocomposite	020	13.48	6.56	0.352	24.2	70.3
	110	16.88	5.25	0.415	20.9	

discussed in previous results which originate from the introduction of ataPHB.

Crystal Structure and Morphology

PHBV can crystallize in either PHB unit cell or PHV unit cell, which depends on the content of HV composition, and the transformation from PHB lattice to PHV lattice occurs at about 30 mol % HV.[4] It has been reported that diffraction peak at $2\theta = 17°$ is associated with the (1 1 0) diffraction of PHB type lattice and at $2\theta = 18°$ is associated with the (0 2 0) diffraction of PHV type lattice.[19] The WAXD results (Supporting Information Figure S2) showed that there was only PHB type lattice existing in both PHBV and nanofiller/PHBV nanocomposites, indicating that the introduction of nanofillers does not affect the basic crystalline structure of PHBV. Crystallinity (X_t) and crystallite size (H_{hkl}) (determined by Scherrer formula) calculated according to the WAXD patterns were listed in Tables I and II. Table I shows the effects of MWCNTs and MWCNTs-PHB contents on the crystallinity of PHBV matrices. With addition of MWCNTs in an amount of 0.1 wt %, the crystallinity of PHBV matrix decreased from 68.9% (for neat PHBV) to 67.5%. In the case of MWCNTs-PHB/PHBV nanocomposite, the crystallinity decreased even when the amount increased to 0.6 wt %. With further addition of nanofillers, the crystallinity of nanocomposites enhanced and reached 77.3% and 72.1% for MWCNTs/PHBV and MWCNTs-PHB/PHBV nanocomposites, respectively, with a nanofiller content of 3 wt %. The trend of crystallinity decreasing at first and then increasing with the increasing amount of nanofillers indicates both retarding and nucleation effects exist in the nanofiller/PHBV nanocomposites. Besides, the retarding effect of MWCNTs-PHB is much stronger than MWCNTs, which is consistent with the DSC results. It is noticed that the crystallite sizes of nanocomposites were larger than that of neat PHBV (shown in Table II). Such behavior has been reported in somewhere else.[22] The elevated crystallinity and crystallite size of nanocomposites assert that nanofillers have a positive effect on the crystallization of PHBV.

Figure 5 shows the typical polarized optical micrographs of PHBV and nanofiller/PHBV nanocomposites with different contents of nanofiller after melt-crystallized at 80°C. The size of PHBV spherulites was large because of the low nucleation density which is resulted from the high purity of PHBV. With the addition of both MWCNTs and MWCNTs-PHB, the spherulite size became smaller because the nucleation density was much higher than that of neat PHBV. The nucleation density of nanofiller/PHBV nanocomposites increased at first and subsequently decreased and then increased again with the increasing of nanofillers content, which kept the same trend as crystallization rate indicated by DSC results. This further improved the heterogeneous nucleation effect and the agglomeration of nanofillers coexisted in the nanocomposites. On the whole, the nucleation sites of MWCNTs/PHBV nanocomposite were more than MWCNTs-PHB/PHBV nanocomposite at the same nanofiller content except 1 wt %, indicating stronger heterogeneous nucleation effect and more serious agglomeration of nanofillers in MWCNTs/PHBV nanocomposite.

Dispersion of Nanofiller in PHBV Matrix

The dispersion of nanofiller in polymer matrix is one of the most important factors for fabricating high performance nanofiller/polymer nanocomposite. A homogeneous dispersion of nanofiller and strong interfacial interaction between polymer matrix and nanofiller can effectively improve the mechanical properties of polymer composites. The dispersions of four types of MWCNTs in nanocomposites with nanofiller content of 1.0 wt % are shown in Figure 6. The distribution of MWCNTs was not uniform in the MWCNTs/PHBV nanocomposite, which was not favorable to enhance the properties of polymer matrix. In contrast to MWCNTs/PHBV nanocomposite, functionalized MWCNTs showed homogeneous distributions in PHBV matrices, indicating better interfacial adhesion between the functionalized MWCNTs and PHBV. The good interfacial adhesion is mainly facilitated by the interactions between the functional carboxyl group, hydroxyl group, and ataPHB on MWCNTs surfaces and PHBV chains.

Dynamic Mechanical and Tensile Properties

In an attempt to examine the reinforcing effects of the nanofillers, the dynamic mechanical properties and tensile properties of neat PHBV and its nanocomposites were studied by DMA and tensile experiment, respectively. Figure 7 and Supporting Information Figure S3 show the storage modulus curves of neat PHBV and its nanocomposites with different contents of

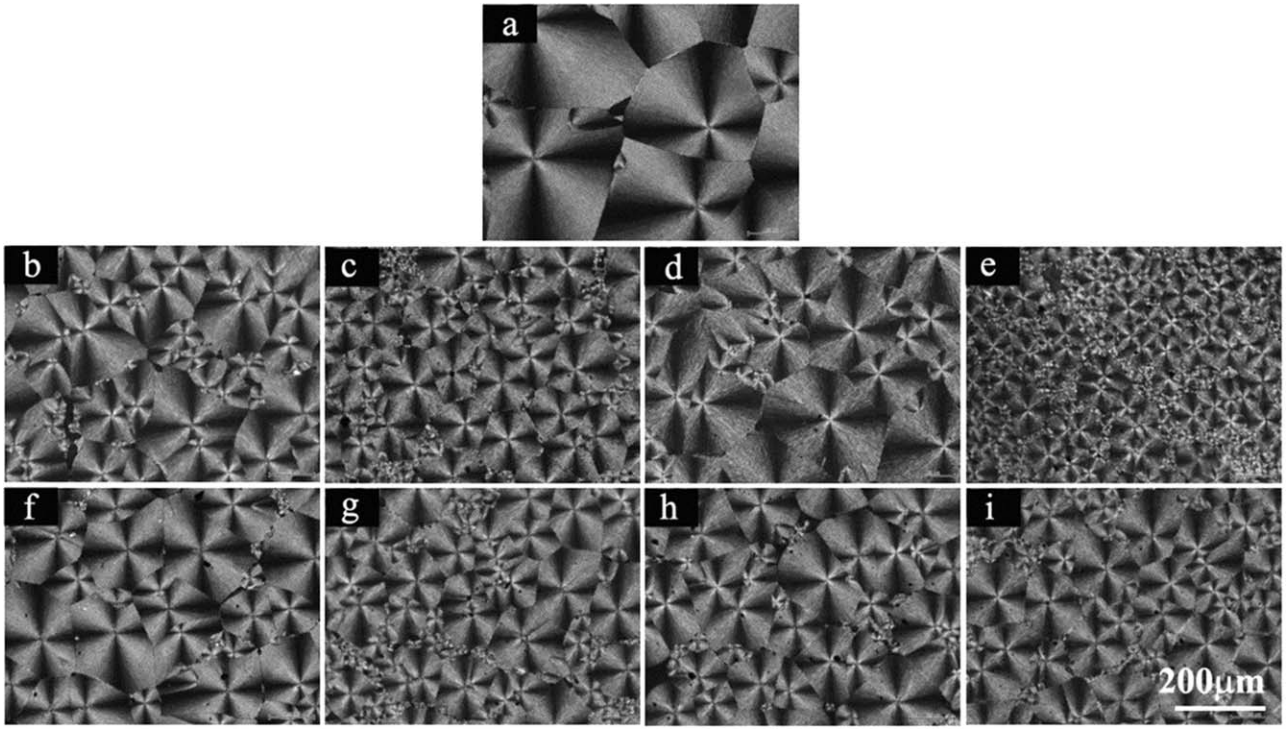

Figure 5. Polarized optical micrographs of neat PHBV (a), MWCNTs/PHBV nanocomposites (b, c, d, and e) and MWCNTs-PHB/PHBV nanocomposites (f, g, h, and i) isothermally crystallized at 80°C, (b, f) 0.1 wt %, (c, g) 0.6 wt %, (d, h) 1 wt %, and (e, i) 3 wt %.

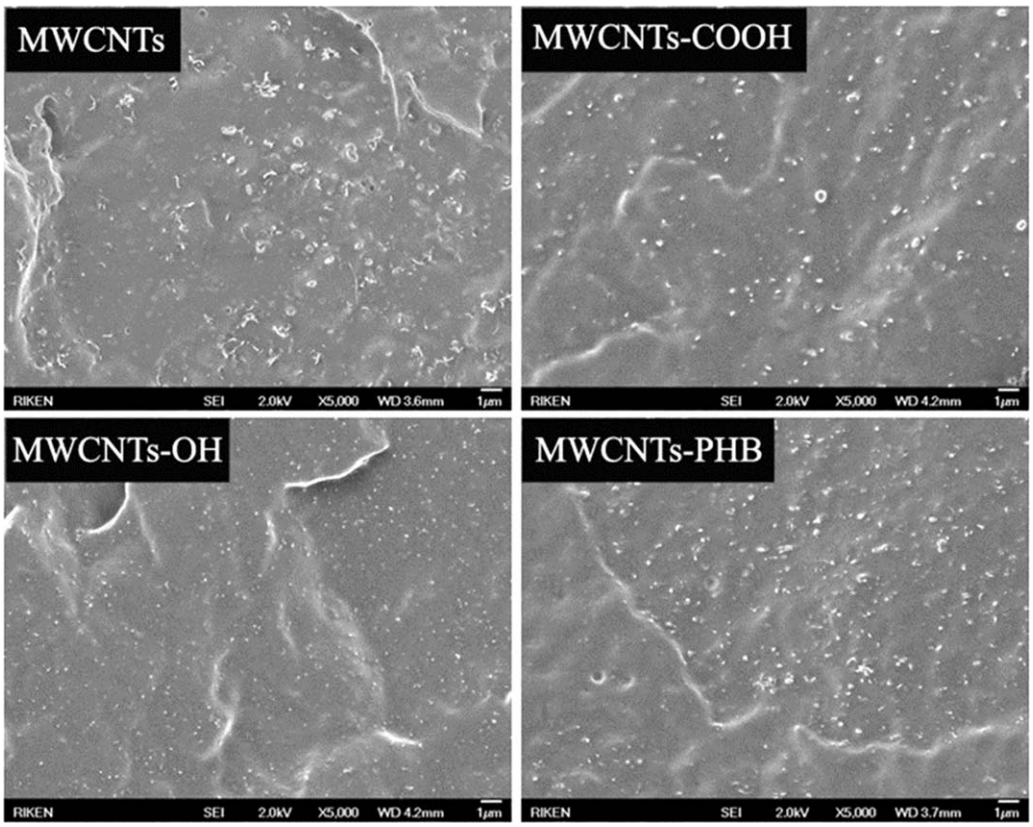

Figure 6. SEM micrographs for nanofiller/PHBV nanocomposites with nanofiller content of 1.0 wt %.

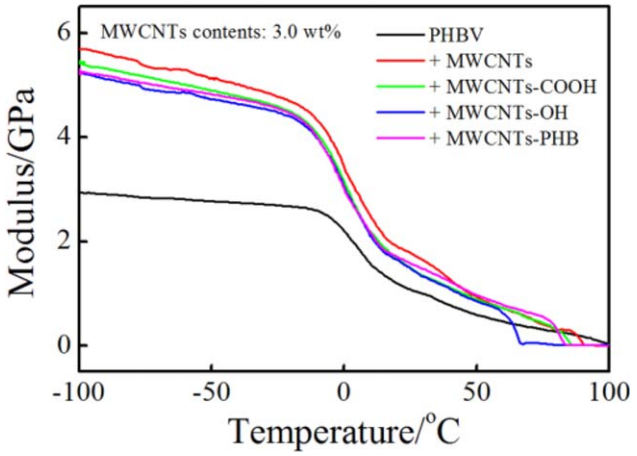

Figure 7. DMA storage modulus as a function of temperature for neat PHBV and its nanocomposites. [Color figure can be viewed in the online issue, which is available at wileyonlinelibrary.com.]

nanofillers. Neat PHBV showed highest storage modulus (E') at the temperature range below its glass transition temperature (T_g). When the temperature increased above its T_g, the E' of PHBV decreased sharply due to the occurrence of glass transition (from 2.9 GPa at −100°C to 1.1 GPa at room temperature). In the case of nanocomposites, the E' increased with increasing content of nanofillers. The E' of nanocomposites with 3.0 wt % nanofillers increased by about 79% from 2.9 ± 1.2 to 5.2 ± 1.6 GPa at −90°C and about 36% from 1.1 ± 0.3 to 1.5 ± 0.4 GPa at room temperature, suggesting that the incorporation of nanofillers significantly enhances the storage modulus of PHBV.

Figure 8 shows the strain–stress curves of neat PHBV and nanofiller/PHBV nanocomposites with 1.0 wt % nanofillers. MWCNTs/PHBV nanocomposite was very brittle with the elongation at break only about 3%. Compared with MWCNTs/PHBV nanocomposite, pure PHBV showed a slightly better flexibility with elongation about 6%, which was similar to functionalized MWCNTs/PHBV nanocomposites. However, the strength

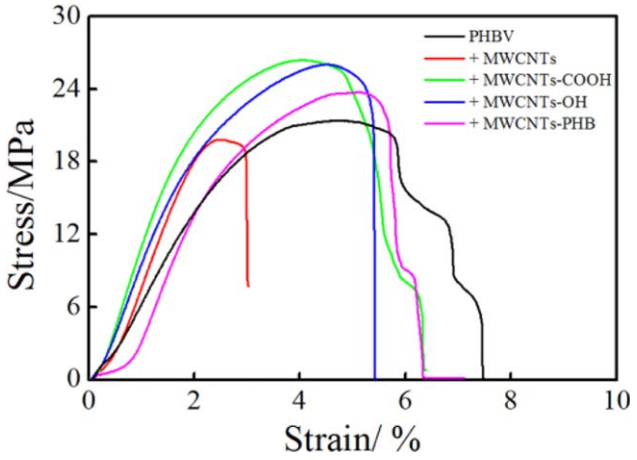

Figure 8. Tensile stress–strain curves of PHBV and its nanocomposites with nanofiller content of 1.0 wt %. [Color figure can be viewed in the online issue, which is available at wileyonlinelibrary.com.]

of PHBV was lower than functionalized MWCNTs/PHBV nanocomposites. The results demonstrate that the presence of a little amount of functionalized MWCNTs improved the mechanical performance of PHBV matrix. It is known that crystallinity influences the tensile strength, but the increase of crystallinity for nanocomposites compared with neat PHBV only ranged from −3 to 5% (shown in Table II). Hence, the improvement of tensile strength for functionalized MWCNTs/PHBV nanocomposites was mainly due to the introduction of the nanotubes. These results indicate that the chemical groups and ataPHB grafted on the surface of the MWCNTs not only facilitate a uniform dispersion of the MWCNTs within PHBV matrices, but also build up a strong interface interaction between functionalized MWCNTs and PHBV. Also the abundant interfacial area at the nanoscale is essential for effective stress distribution and stress transfer between functionalized MWCNTs and PHBV matrices.

CONCLUSION

MWCNTs functionalized with carboxyl groups, hydroxyl groups, and ataPHB were successfully obtained through acid oxidation, esterification reaction, and "grafting from" method, respectively. Both MWCNTs and the three types functionalized MWCNTs were used to fabricate nanofiller/PHBV nanocomposites. The melting and crystallization behaviors of PHBV and its nanocomposites have been investigated in this study. On one hand, the four types nanofillers act as the heterogeneous nucleation agents for PHBV and thereby improve the crystallization rate. On the other hand, more steric hindrance introduced by nanofillers limits the mobility of PHBV chains, which is not favorable to the crystallization. In addition, more nanofillers especially MWCNTs could induce agglomeration of nanofillers in nanocomposites, resulting in decreased amounts of heterogeneous nucleation sites. The incorporation of nanofillers induced the increase of crystallinity and crystallite sizes of PHBV, while the basic crystalline structure of the PHBV was not influenced. Based on the SEM results, it is concluded that functionalized MWCNTs led to an enhanced interfacial interaction between nanofiller and PHBV, which dramatically improved the dispersion of nanofillers in PHBV matrix. Furthermore, functionalized MWCNTs improved the strength of nanocomposites while maintaining the toughness.

REFERENCES

1. Schlegel, H. G.; Gottschalk, G.; Bartha, R. V. *Nature (London)* **1961**, *191*, 463.
2. Rho, J. K.; Choi, M. H.; Gutierrez, M.; Tian, B. X.; Yoo, T.; Baek, J. E.; Shah, M.; Yoon, S. C. *J. Appl. Polym. Sci.* **2014**, *131*, 41074.
3. Bluhm, T. L.; Hamer, G. K.; Marchessault, R. H.; Fyfe, C. A.; Veregin, R. P. *Macromolecules* **1986**, *19*, 2871.
4. Catoni, S. E. M.; Trindade, K. N.; Gomes, C. A. T; Schneider, A. L. S.; Pezzin, A. P. T. *Polímeros* **2013**, *23*, 20.
5. Vidhate, S.; Innocentini-Mei, L.; D'Souza, N. A. *Polym. Eng. Sci.* **2012**, *52*, 1367.

6. Carli, L. N.; Daitx, T. S.; Guegan, R.; Giovanela, M.; Crespo, J. S.; Mauler, R. S. *Polym. Int.* **2015**, *64*, 235.
7. Javadi, A.; Srithep, Y.; Pilla, S.; Clemons, C. C.; Gong, S. Q.; Turng, L. S. *Polym. Eng. Sci.* **2011**, *51*, 1815.
8. Wang, S. F.; Song, C. J.; Chen, G. X.; Guo, T. Y.; Liu, J.; Zhang, B. H.; Takeuchi, S. *Polym. Degrad. Stab.* **2005**, *87*, 69.
9. Iijima, S. *Nature* **1991**, *354*, 56.
10. Sachdev, V. K.; Bhattacharya, S.; Patel, K.; Sharma, S. K.; Mehra, N. C.; Tandon, R. P. *J. Appl. Polym. Sci.* **2014**, *131*, 40201.
11. Wang, K.; Li, N.; Ren, K.; Zhang, Q.; Fu, Q. *Compos. Part A: Appl. Sci. Manuf.* **2014**, *61*, 84.
12. Díez-Pascual, A. M.; Naffakh, M. *Compos Part A: Appl. Sci. Manuf.* **2013**, *54*, 10.
13. Coleman, J. N.; Khan, U.; Blau, W. J.; Gun'ko, Y. K. S. *Carbon* **2006**, *44*, 1624.
14. Abe, H.; Doi, Y.; Satkowski, M.; Noda, I. *Macromolecules* **1994**, *27*, 50.
15. Pearce, R.; Jesudason, J.; Orts, W.; Marchessault, R. H.; Bloembergen, S. *Polymer* **1992**, *33*, 4647.
16. Pearce, R.; Brown, G. R.; Marchessault, R. H. *Polymer* **1994**, *35*, 3984.
17. Abe, H.; Matsubara, I.; Doi, Y. *Macromolecules* **1995**, *28*, 844.
18. Scandola, M.; Focarete, M. L.; Adamus, G.; Sikorska, W.; Baranowska, I.; Swierczek, S.; Gnatowski, M.; Kowalczuk, M.; Jedlinçski, Z. *Macromolecules* **1997**, *30*, 2568.
19. Gunaratne, L.; Shanks, R. A. *Eur. Polym. J.* **2005**, *41*, 2980.
20. Yang, Z. P.; Lu, H. B. *J. Appl. Polym. Sci.* **2013**, *128*, 802.
21. Pan, P. J.; Shan, G. R.; Bao, Y. Z.; Weng, Z. X. *J. Appl. Polym. Sci.* **2013**, *129*, 1374.
22. Shan, G. F.; Gong, X.; Chen, W. P.; Chen, L.; Zhu, M. F. *Colloid Polym. Sci.* **2011**, *289*, 1005.